PRODUCTION AND CHARACTERISATION OF INVERSE COMPTON SCATTERING X-RAYS WITH A 17 MEV ELECTRON BEAM

A.S. Chauchat *, V. Le Flanchec, J.P. Nègre, A. Binet
CEA DAM DIF, F-91297 Arpajon, France
J.P. Brasile
THALES Communication, 160 Bd de Valmy, F-92700 Colombes, France
J.M. Ortega
CLIO/LCP, Bâtiment 201, Université Paris-Sud, F-91450 Orsay, France

Abstract

Inverse Compton scattering is a well-known process to produce X-rays. Thanks to recent progress in accelerators and laser field, such sources have been developed worldwide. The ELSA linear electron accelerator (CEA DAM DIF, Arpajon, France) just developed its own source. The 17 MeV electron beam interacts with a 532 nm laser to provide a pulsed 10 keV X-ray source. The X-ray beam profile is observed on radio-luminescent imaging plates. In order to increase the signal to noise ratio of this X-ray source, laser developments are in progress.

INTRODUCTION

ICS (Inverse Compton Scattering) is on the way to bring to X-ray application field a new X-ray production mode. High brightness flux, energy tune-ability and high monochromaticity are the main advantages of this source. Moreover, the compactness of the production system should allow the users to possess their own source. Before developing a full scale machine, experimentations are necessary to evaluate the technical needs. The ELSA facility located at the CEA DAM DIF (France) fits the needs for this type of evaluation [1]. ELSA is a high-brightness 1-18 MeV electron source using a laser driven photo-injector. As former free electron laser [2], the accelerator provides a low emittance electron beam which is one of the necessary features to efficiently produce X-rays. As a 72.2 MHz Nd:YAG laser is used to produce electrons, it's convenient to derive this laser line to produce the synchronous photons that interact with the electron beam. The X-ray photons resulting from the interaction between electron and laser beam are detected by radio-luminescent imaging plates. This detector gives a nice image of the beam angular distribution but is not appropriate to evaluate the number of emitted photons. To use other detectors, it's necessary to increase the signal to noise ratio of the X-ray flux. In this paper, we describe the new laser set-up used to increase the peak power density in a few pulses instead of spreading the low energy on 1444 pulses like it was done in [3].

* anne-sophie.chauchat@cea.fr

INVERSE COMPTON SCATTERING

The ICS process can be seen from two different viewpoints. It can be either described as the interaction between two particles, photon and electron using the elasticity property of the collision, or as the radiation of electrons in the electromagnetic field of the laser. In both cases, theory shows that photons are emitted in a narrow cone in the direction of the electron beam with a higher energy than the incident laser energy. With the values of electron energy and the laser power involved in this experiment, it's convenient to use formula from the electron-photon collision theory (Figure 1).

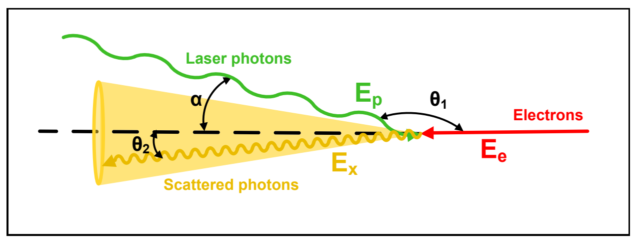

Figure 1: Scheme of the inverse Compton interaction seen as electron-photon collision.

In the special case of head-on collision between the two beams ($\alpha = 0$), maximal X-ray energy is obtained for $\theta_2 = 0$ by formula (1):

$$E_X = 4\gamma^2 E_p \tag{1}$$

Formula (1) shows clearly the tune-ability of the source function of electron (by the relativistic γ factor) and incident photon energy. The interaction cross section calculated by the relativistic invariants [4] is proved to be close to the Thomson cross section: $\sigma_{Th} = \frac{8\pi r_e^2}{3} = 6.65 \times 10^{-29}\mathrm{m}^2$. An approximation of the scattered photon number is given by formula (2):

$$N_X = \frac{N_e N_p \sigma_{Th} f_{rep}}{4\pi s^2} \tag{2}$$

where N_e, N_p are the numbers of electrons and photons, f_{rep} the repetition frequency of the collision and s the interaction section. High photon flux is provided by high repetition frequency and high beam intensity. The differential cross section of the interaction $\frac{d\sigma}{d\Omega}$ shows that most of the X-ray flux is concentrated in a $\frac{1}{\gamma}$ half angle cone whose symmetry axis is in the electron beam direction (Figure 2).

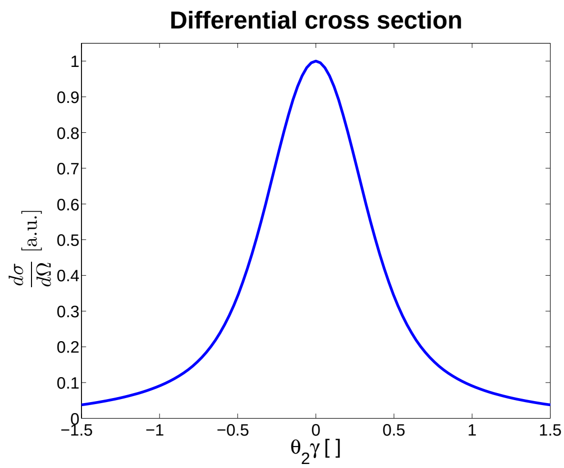

Figure 2: Differential cross section as a function of observation angle in units of $\frac{1}{\gamma}$

X-RAY SOURCE IMAGING

Beam parameters

First ICS experiments on the ELSA facility consisted in working on spatial and temporal diagnostics to manage the beam overlapping and observe the X-ray beam profile. We chose a 20 μs train of laser and electron pulses at 72.2 MHz i.e. 1444 pulses at 1 Hz repetition rate. ELSA laser system produces both photons for the photo-injector and for the "Compton laser line". The laser consists of a diode-pumped Nd:YAG mode-locked oscillator at 72.2 MHz producing 35 ps pulses, followed by a pulse selector and a Nd:YAG amplifier chain described in-depth in [5]. The pulse selector is used to create macropulses. Then the laser beam is split between two lines. On the "Compton line" an extra double-pass Nd:YAG amplifier (12 mm diameter) increases the laser power before being converted. On the "photo-injector line", the beam is directly converted from 1064 nm to 532 nm by a KTP frequency doubling crystal (12 x 12 x 20 mm^3). With this system we had 300 mJ green macropulses for the Compton line. A retractable aluminum bevel-edge is used to temporally and spatially visualize the beam overlapping. A side of the bevel-edge is polished to act as an Optical Transition Radiator, the other side diffuses the laser beam to the cameras. A CCD camera and a streak camera recover the visible light from the beams. The timing between the bunches is tuned by an optical variable delay line inserted in the Compton laser line. Table 1 sums up the experiment parameters.

Table 1: Beam parameters

Electron beam parameters
Energy (electron): 17 MeV
Charge (pulse): 0.2 nC
Transverse radius (pulse): 100 μm (h) 80 μm (v)
Laser beam parameters
Wavelength: 532 nm
Energy (pulse): 200 μJ
Transverse radius (pulse): 40 μm (h) 65 μm (v)

X-ray beam profile

Careful beam focusing and accurate synchronization were required to produce X-rays. For the detection we used photostimulated Imaging Plates from Fujifilm Company. They consist of a flexible plastic substrate covered by a 115 μm thick layer of radiosensitive BaF(Br,I):Eu^{2+} crystals combined in an organic binder. After exposure, the plate is stimulated by a 650 nm wavelength laser so that the phosphor layer emits photons by stimulated luminescence. The intensity of these emitted photons is proportional to the deposited dose in the radiosensitive layer. An acquisition software displays the image in grey levels. The pixel intensity is stated in an arbitrary unit: PSL (Photo-Stimulated Luminescence). On Figure 3 we compare the Imaging Plate without Compton laser (left side) where we only see the background noise, and the Imaging Plate radiated by "Compton" X-rays. The X-ray signal is collimated by the 40 mm diameter beryllium window which separates vacuum from air.

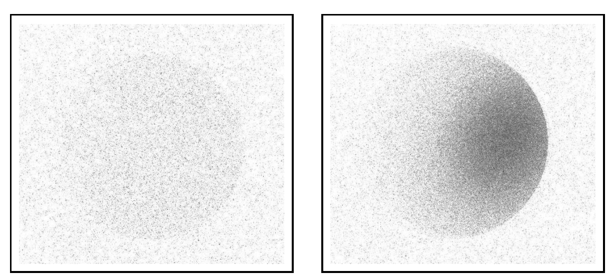

Figure 3: Imaging plates: background noise (left) X-ray signal (right).

Signal analysis

With the acquisition and processing software used for the imaging plates, we can get the image vertical profile in PSL arbitrary unit (Figure 4). The gaussian plot fitted to the signal has a 9.8 mm standard deviation. The fact that the experimental plot does not fit the gaussian plot on the lower part of the signal is due to the collimation by the 40 mm diameter beryllium window. Analysing the gaussian plot, we note that 99% of the signal is emitted in a 30 mrad half angle cone.

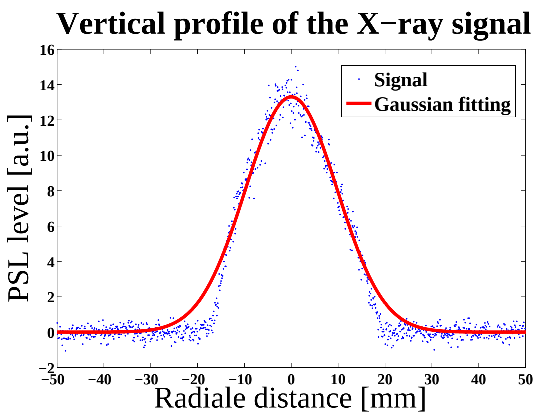

Figure 4: Difference between X-ray signal and background noise, with a gaussian fitting.

To have an idea of the number of emitted photons, we need to calibrate the imager (imaging plate+scanner). With the Monte-Carlo code MCNP5, we simulate the photons behavior from the source point to the radiosensitive layer of the Imaging Plate, we obtain plots of the number of photons absorbed by the phosphor layer function of photon energy. Then, by calibration measurements with standard X-rays source (5.5 keV X-ray tube and 1 MeV ^{60}Co) we obtain plots of the imager sensitivity in PSL/mm^2/photon function of X-ray photon energy. As we know theoretically the photon energy function of its scattering angle, we can deduce from the imager sensitivity, the number of emitted photons. In the [-10 mm; 10 mm] range, we estimate the number of emitted photons to be 3.4×10^3 photons/s. The average flux in the $\frac{1}{\gamma}$ = 30 mrad half-angle cone is 5.4×10^3 photons/s. The average brightness of the source is 4.2×10^3 photons/s/mm^2/mrad^2/10%BW. In order to better understand the experiment, I use a Monte-Carlo code CAIN to find by modelling the number of emitted photons. The code runs with 100 000 macroparticles and beam parameters from table 1. With CAIN, it's possible to implement the code with a beam transport code to accurately modelize the Twiss parameters of the electron beam at the interaction point. The CAIN code gives a result file with the position and energy of emitted photon macroparticles. From this file, we plot the X-ray beam profile such as the one got with the imaging plate processing software. We compare directly the experimental result with the number of photons on the beam profile. We found with the calculation 2.6×10^3 photons/s in the [-10 mm; 10 mm] range. This result is very close to the experimental result.

NEW LASER SETTING-UP

The drawback of this X-rays production process is the low interaction cross-section. To get a better signal, we have to increase the particles density without increasing the background noise. As the main background noise is due to the radiation of lost electrons on the vacuum tube, we decided to act on the laser line. The idea is to store the whole macropulse laser energy (300 mJ, 1444 pulses) in a small number of pulses (typically 20 pulses or less). Laser peak power increases and there is no more lost electrons. The only limitation we have is the damage threshold of optical surfaces. To store such a high energy into a few pulses, we need to inject as much pump power as possible into our Nd:YAG amplifier, which creates Amplified Spontaneous Emission (ASE). It leads to parasitic oscillations that degrade our picoseconds pulses train, and can also damage the amplifier and doubling crystal. We removed all parasitic oscillation by adding a Pockels cell based shutter (3 ns rise and fall time) upstream of the two stages Nd:YAG amplifier. Reduction of the ASE is necessary to preserve a good conversion yield in the doubling crystal and avoid the so-called "gray-tracking" effect inside the KTP. One of our crystals was damaged by gray-tracking but the gray-tracked crystals partially recover after a few minutes. With this new system, we were able to produce laser macropulses composed of 20 pulses with 50 mJ with a conversion yield in the doubling crystal of 45 %. We can hope to gain at least a 10 factor in the signal to noise ratio.

CONCLUSION

We succeeded in producing 10 keV energy X-ray beam by Inverse Compton Scattering. The use of radioluminescent Imaging Plates was mandatory to visualize the cone space distribution of the X-ray beam. An improvement in the laser system brings a 10 factor to the laser peak power. These should increase the signal to noise ratio and allow the use of real-time X-ray detectors, experiments are in progress. In addition to detectors characterisation, the goal of this source is to validate some calculation codes on Inverse Compton Scattering to the design of a full-fledged X-ray compact source.

REFERENCES

[1] A.S. Chauchat et al., Construction of a Compton source for X-rays in the ELSA facility, NIM A 608 (2009) S99-S102.

[2] S. Joly, Progress report on the ELSA FEL and first lasing, NIMA 331 (1993) 199-203.

[3] A.S. Chauchat et al., Instrumentation developments for production and characterization of Inverse Compton Scattering X-rays and first results with a 17 MeV electron beam, submitted to NIMA.

[4] L. Landau and E.M. Lifchitz, Course of theoretical physics, Vol. 4, Part. I, Relativistic Quantum Mechanics, Pergamon 1971.

[5] V. Le Flanchec, Output energy fluctuations of the Nd:YAG amplifier chain of a photoinjector drive laser system, Applied Optics, Vol. 37, No. 27, September 1998.